Performance Enhancement of Single-Chamber Sediment-Microbial Fuel Cell with Variation in Cathode Surface Area

H.C. Teng*‡, B.C. Kok*, C. Uttraphan**, M.H. Yee***

*Department of Electrical Power Engineering, Faculty of Electrical and Electronic Engineering, Universiti Tun Hussein Onn Malaysia, 86400 Parit Raja, Batu Pahat, Johor.

** Department of Computer Engineering, Faculty of Electrical and Electronic Engineering, Universiti Tun Hussein Onn Malaysia, 86400 Parit Raja, Batu Pahat, Johor.

*** Department of Engineering Education, Faculty of Technic and Vocational Education, Universiti Tun Hussein Onn Malaysia, 86400 Parit Raja, Batu Pahat, Johor.

(ge170107@siswa.uthm.edu.my, bckok@uthm.edu.my, chessda@uthm.edu.my, mhyee@uthm.edu.my)

‡H.C. Teng; B.C. Kok, Department of Electrical Power Engineering, Faculty of Electrical and Electronic Engineering, Universiti Tun Hussein Onn Malaysia, 86400 Parit Raja, Batu Pahat, Johor,

ge170107@siswa.uthm.edu.my

Received: 21.02.2020 Accepted:18.03.2020

Abstract- This study investigates the impact of cathode surface area on single chamber sediment-microbial fuel cell (S-MFC). A fixed graphite anode surface area of 0.000471m^2 has been used on four S-MFCs coupled with four carbon fiber cloth cathode electrodes with variation of surface area. Pond sediment has been used as the anode medium that inoculated with acetate as substrate to ramp up the amount of electrochemical-active bacteria (EAB). The S-MFCs has been operated and monitored for 120 hours using Arduino based data logger. The outcomes of this observation period have indicated the S-MFC with larger cathode surface area (0.01m^2) possess smaller internal resistance (123.96±2.68 Ω) and thus performed significantly better than other S-MFC with the smaller cathode surface area, resulting with average voltage and current of 0.598±0.008V and 4.827±0.124mA respectively, where a maximum power density of 2.867mW with a coulombic efficiency of 64.63% was achieved. Successful performance increase suggests enlargement of the cathode area could be the alternative to reduce the internal resistance in traditional MFCs for electricity generation.

Keywords Sediment-Microbial Fuel Cell; Cathode Surface Area; Internal Resistance; Increased Performance; Coulombic Efficiency.

1. Introduction

Sediment microbial fuel cell (S-MFC) is an iteration from the traditional microbial fuel cell (MFC) which uses waste organic sediment as anode medium. It can be viewed as new type of renewable energy [1]–[5] as all living creatures producing waste products during their life cycle in the functions of living in which it is typically being discarded on the land and water. This excreted organic waste degrades and dissipates into the microorganism-rich surrounding [6]–[11]. Consequently, electrical energy can be harvested by taking the advantage of the microbe metabolism in the sediment. With determination, several researchers [12]–[14] have established S-MFC which comprises of an anode electrode rooted in anaerobic residue and cathode electrode placed in the aerobic water reservoir above the anode electrode. Electrochemical-active bacteria (EAB) transmits electrons to the anode electrode during oxidation of the organic compound while the electrons are accepted by a cathode and thus, reducing the oxygen around it to become

water [15]. Subsequently, the electrons movement generates electric current.

In an S-MFC, sediment is viewed as both substrate and inoculum. Every sediment type has their own characteristic such as conductivity, porosity, etc. Regardless the type of sediment used, the internal resistance of S-MFC plays an important role in the overall system performance [16]–[18]. Hence, several configurations of S-MFC were developed to improve and tackle the restrictions [19]–[26]. Moreover, reduction in internal resistance means that the system is able to supply more power density and reduction in internal losses. Air-cathode MFCs that usually operates in membrane-less configuration have low overall cost, simpler design, and relatively high-power density. However, the gap between anode and cathode of the air-cathode MFCs is limited [27], while there are possible voltage reversal [25] due to the unstable reaction in the presence of oxygen in anode compartment that might destroying the anode biofilm or even the electrode materials [28].

In this study, four single-chamber S-MFCs with different cathode surface area have been developed based on the microbial reaction in a controlled room temperature. The developed S-MFCs are first inoculated in order to maximize the amount of EAB presented in the sediment, coupled with cellulose membrane to prevent the oxygen diffusing into anode to cause voltage reversal [25]. The goals of this work are to compare and investigate the effects of the cathode surface area on the performance of the S-MFC.

2. Materials and Method

2.1. S-MFC Architecture and Operation

Four single-chamber MFC have been prepared in squared-cube glass jars measuring (0.1 × 0.1 × 0.1m) with an inner volume of 0.001m^3, ignoring the rounded corners and the jar lids. Medium used in anode compartment is the marine sediment retrieved from the pond opposite of Faculty of Technology Management and Business, Universiti Tun Hussein Onn Malaysia (UTHM) (1.86262°N 103.08126°E). The anode electrode is a graphite rod (surface area of 0.000471m^2), while carbon fiber cloth act as air cathode electrode. Each single-chamber MFC's anode electrode is embedded in 50g of marine sediment and wrapped in a cellulose fiber membrane with a surface area of 0.01m^2 facing cathodic compartment. Ethylene Propylene Diene Monomer (EPDM) rubber tube is then embedded to the anode medium for channeling anode electrode pin-out and also works as feeding channel for anode medium. The cathode electrodes are cut in different area sizes as shown in Table 1 which are then positioned on the exterior surface of the membrane as close as possible. The distance between the anode and the cathode is approximately 5cm apart. Carbon fiber strand is used to connect the circuit. The glass chambers and rubber tubes are then sealed using a jar cap and hot glue gun except the rubber tube that houses the cathode electrode to allow air flow. The setup is illustrated as in Fig. 1.

Table 1. Cathode dimension for each S-MFC

S-MFC No.	Cathode Dimension (Surface area)
1	0.1 m x 0.1 m (0.01 m^2)
2	0.075 m x 0.075 m (0.005625 m^2)
3	0.05 m x 0.05 m (0.0025 m^2)
4	0.025 m x 0.025 m (0.000625 m^2)

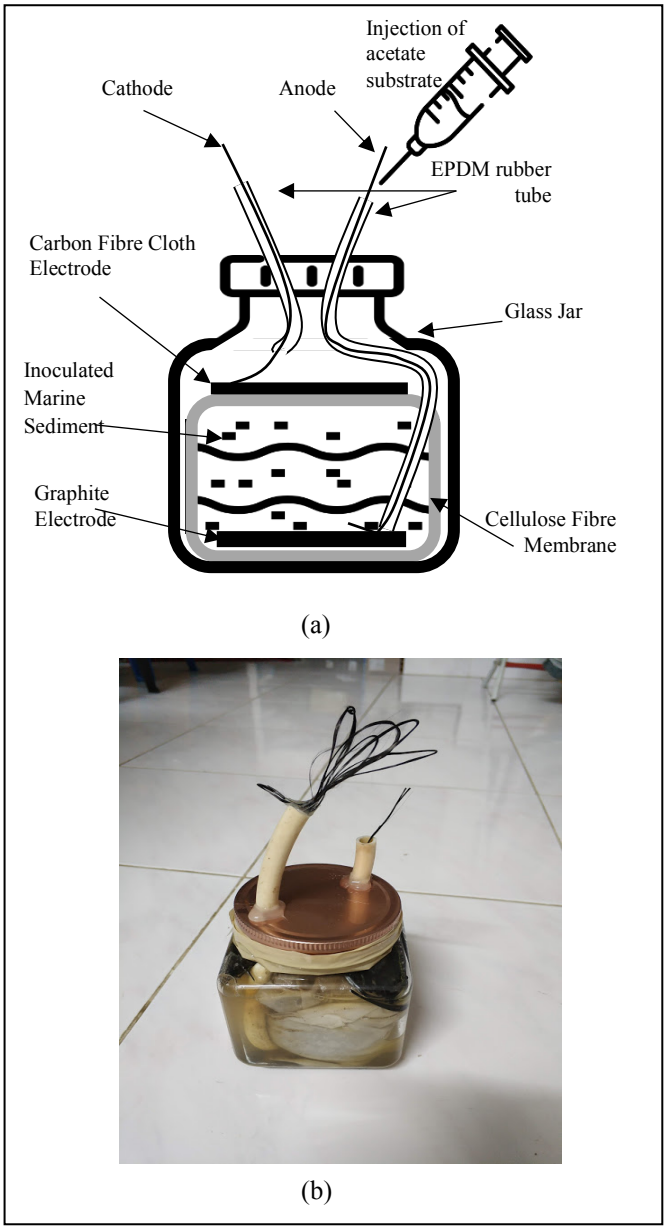

Fig. 1. (a) 2-D scheme of the single-chamber S-MFC (b) Constructed S-MFC

The wastewater sludge from the pond is used as the inoculum of the anode medium, each chamber is fed with 20ml of salt solution containing 2400mg/L (0.04M) acetate substrate. This procedure is to shorten the start-up time of the MFC [29]. Within 140 hours of inoculation, the power generation of each S-MFC are being stabilized. Another 20ml of salt solution containing 1000mg/l acetate solution will be injected into each S-MFC before the parallel experiments can be conducted. The specimens are then incubated at a constant room temperature of 30°C. The

current and the voltage are monitored and recorded every hour using Arduino based monitoring system integrated with ACS712 current sensor and HTU21D humidity/temperature sensor that has been developed in advance for 120 hours as shown in Fig. 2.

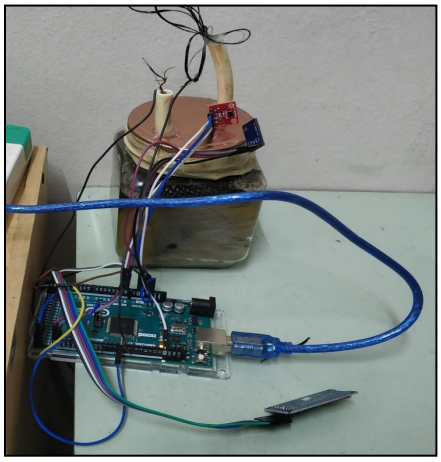

Fig. 2. Data acquisition using Arduino system

2.2. Determination of Internal Resistance of S-MFC

The system is monitored using Arduino data acquisition system which recording the voltage and the current for every one hour. The recorded data is then be plotted in order to determine the trend and characteristics of the S-MFC in controlled room temperature. Subsequently, the internal resistance (R_i) of S-MFC is determined by using Equation (1) and it is then plotted against the cathode cross-section surface area.

$$R_i = \frac{V_{sc}}{I_{sc}} \tag{1}$$

Where V_{sc} is the short circuit voltage (V) and I_{sc} is the short circuit current (A). Then, the energy accumulated was calculated to estimate the energy loss to the surrounding by using Equation (2):

$$E_{acc} = \sum_{i=1}^{T} Pt_i \tag{2}$$

Where P is power, T is total time and t is the time taken in seconds (s).

2.3. Deducing Power Density of S-MFC

In order to obtain the power density curve, the resistor ranging from 100Ω to 22kΩ are being used as an external load which is shown in Table 2. The stable recording of voltage and current are only obtained after 5 – 10 minutes. The power (P) generated in the system can be calculated using the following Equation (3):

$$P = VI \qquad \text{and} \qquad V = IR \tag{3}$$

Where V is the measured voltage (V), I is the current measured (A), and R is the resistance (Ω). Assuming the acetate was completely utilized to generate electricity, the reaction can be written as:

$$CH_3COO^- + 4H_2O \rightarrow 2HCO_3^- + 9H^+ + 8e^- \tag{4}$$

Coulombic efficiency (CE%) [30] is then calculated as in Equation (5), where C_{EX} is the total coulombs calculated with integration of current measured over time interval (i), and C_{Th} is the theoretical amount of coulomb from acetate.

$$CE\% = \left[\frac{C_{Ex}}{C_{Th}}\right] \times 100\%, \tag{5}$$

$$C_{Ex} = \sum_{i=1}^{T} \left[\frac{V_i}{R}\right]_{t_i} \tag{6}$$

$$C_{Th} = FbMv \tag{7}$$

Where F is the Faraday constant (*96485 C mol^{-1}*), b is the number of electrons produced per mol of the substrate (*8 mol/mol acetate*), M is the acetate substrate concentration (*mol/l*) and v is the volume of liquid (*l*).

Table 2. Resistor values used for power density estimation

Resistor value (Ω)
100
330
470
1000
1500
2200
3300
4700
10000
22000

3. Results and Discussion

3.1. Power Generation of S-MFC

Upon the injection of 20 ml of the acetate salt solution, the S-MFC voltage is started to rise until a stable voltage. By plotting the voltage in time domain, it can be seen that S-MFC 1 with higher cathode surface area produces higher voltage, followed by S-MFC 2, S-MFC 3 and S-MFC 4. The obtained results are depicted in Fig. 3.

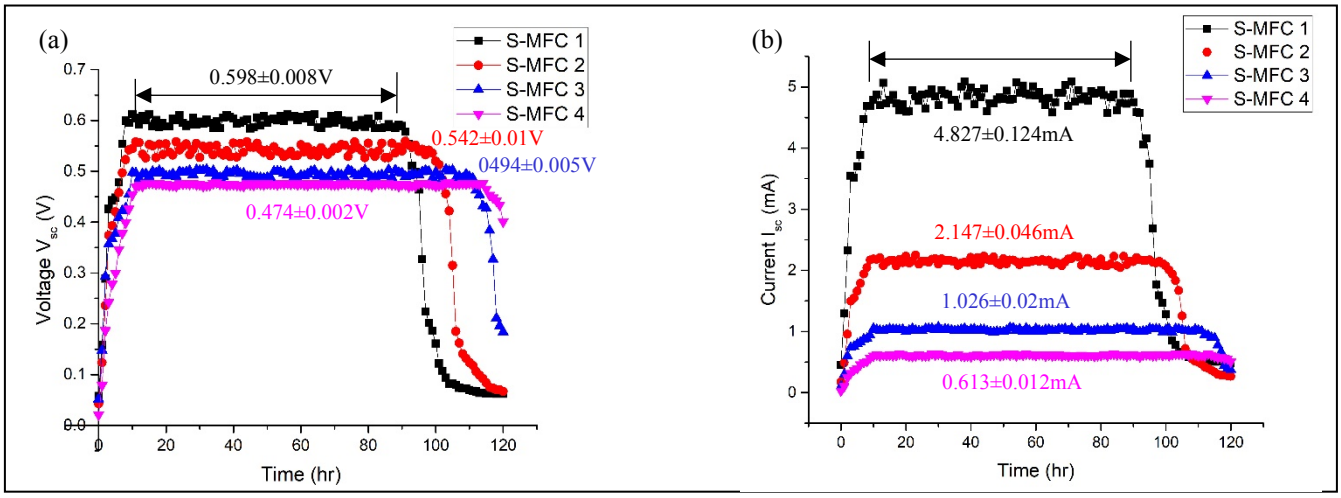

Fig. 3. Electrical generation with 0.04M acetate, where lines show the data range for calculating the average maximum and standard deviation (Avg±SD) for (a) Voltage and (b) Current versus time with their average respect to the legend colour

The voltage and the current trend of all S-MFC exhibits the same trend. However, it can be seen that S-MFC 1 with the largest electrode surface area produces higher voltage and current, but with more obvious stability problems. The voltage and current of S-MFC 1 dropped faster than other S-MFC as it depleted the acetate substrate faster [31]. The total accumulated energy is then calculated using Equation (2) to predict the total energy consumed as well as the losses by the S-MFC. The accumulated energy for all S-MFCs are given in Fig. 4.

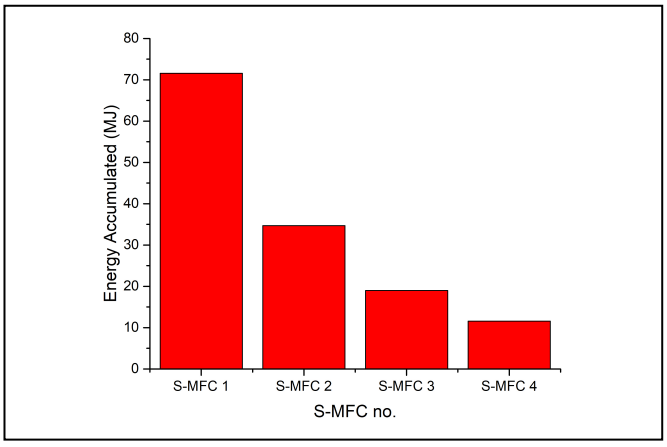

Fig. 4. Total energy accumulation by S-MFC

By referring the S-MFC 4 accumulated energy as the base, it can be seen that the energy accumulated in S-MFC 1 is 619.73% higher than S-MFC 4, while S-MFC 2 and S-MFC 3 are both 300.64% and 164.60% higher than S-MFC 4, respectively. It can be concluded that the possibility of energy loss to surroundings is higher in S-MFC with lower cathode surface area.

3.2. Internal Resistance Reduction Methods

To further investigate the effects of cathode surface area (0.01 m^2, 0.005625 m^2, 0.0025 m^2, and 0.000625 m^2), the power and internal resistance are then plotted as described in Fig. 5.

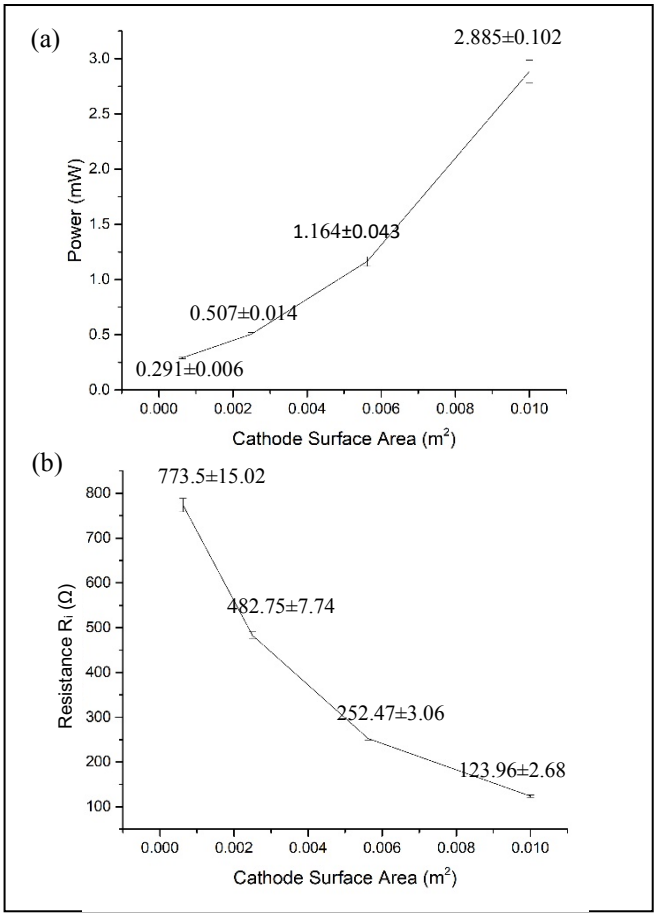

Fig. 5. (a) Power generation and (b) Internal resistance as a function of cathode surface area with error bars integrated into the graph (±SD)

As shown in Fig. 5(a) and Fig. 5(b), it can be deduced that the increment in surface area of cathode leads to the reduction in internal resistance, wherein promotes an increment in power generation of S-MFC. In MFC field, the internal resistance (R_i) is a parameter that indicates the general resistance of the reactor which indirectly specifies the performance of MFC. There are several ways to reduce the internal resistance, both structural and non-structural

methods such as decreasing the distance between anode and cathode, increase the membrane surface or increase the electrode surface area. As expected from the experiment, the increment of cathode area had reduced the internal resistance by significant amount. As instance compared the S-MFC 4 (773.5±15.02Ω) with the S-MFC 1 (123.96±2.68), the internal resistance has reduced about 624%. Instead, there is possibility to reduce further the internal resistance by adding a buffer to the anode medium so as to increase the conductivity.

Deducing the coulombic efficiency using Equation (5), the highest efficiency is obtained from S-MFC 1 (64.63%), followed by S-MFC 2 (31.53%), S-MFC 3 (16.89%) and S-MFC 4 (10.39%). Fig. 6 shows the impact of cathode surface area to the coulombic efficiency based on the experimental results.

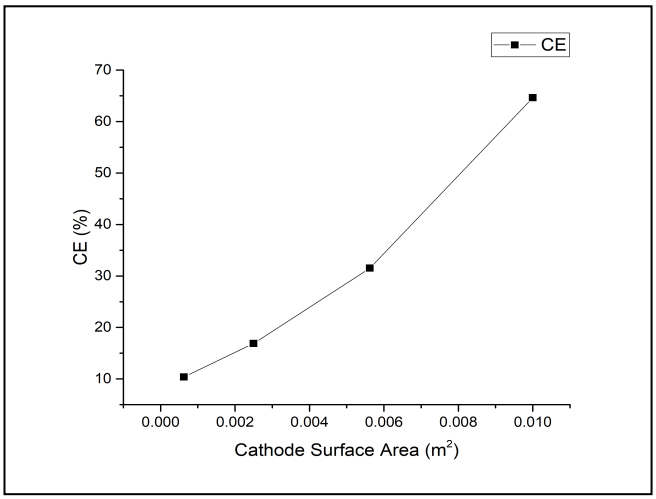

Fig. 6. Coulombic efficiency of S-MFC with different cathode surface area

3.3. Power Density by Limiting the Cathode Surface Area

The characterization of power density produced by S-MFC system can be determined by using fixed load, which varies between 100Ω to 22kΩ. Nevertheless, the results obtained did not certainly the maximum power attainable by each of the S-MFC system.

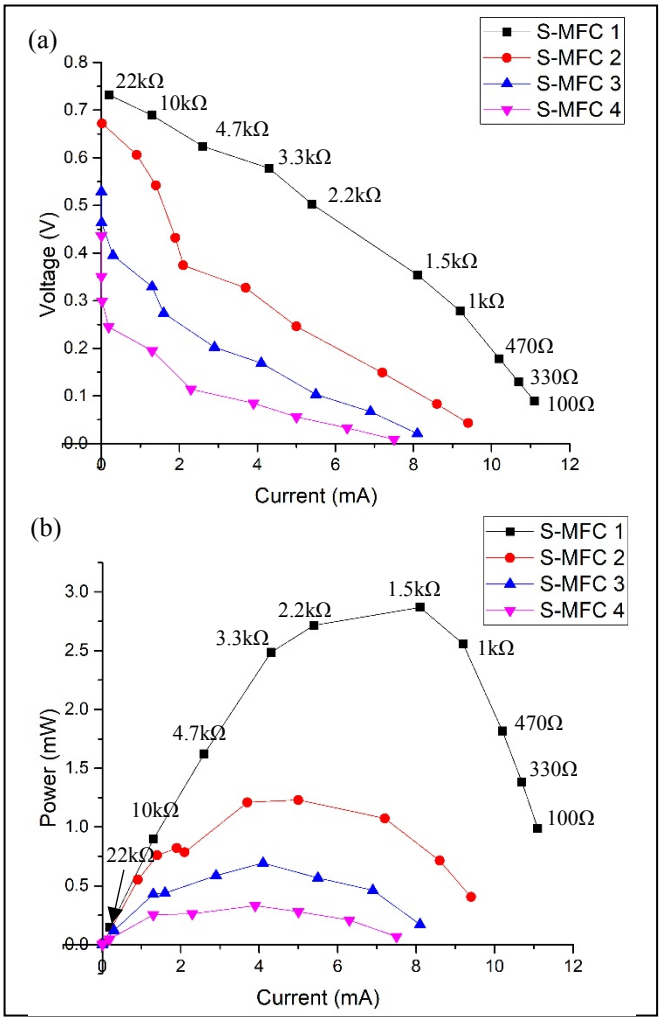

Fig. 7. (a) Voltage and (b) power generated from the characterization test using ten resistors, value ranging from 100Ω – 22kΩ shown in graph.

Referring to Fig. 7(a), the increment in the load leads to the amplification of the voltage and the decrement of the current. For each S-MFC, the maximum power density is obtained when 1.5kΩ resistor is used in the S-MFC 1 (2.867mW) and 1kΩ resistor is used in S-MFC 2 (1.23mW), S-MFC 3 (0.693mW) and S-MFC 4 (0.332mW) (refer to Fig. 7(b)).

4. Conclusion

This study has attempted to employ alternative method in reducing the internal resistance of S-MFC regardless of the anode medium. The placement of the cellulose fiber membrane layer can excellently forbid the diffusion of oxygen from the cathode to the anode while retaining the permeability of hydrogen ion to the cathode. Besides, the utilization of membrane can prevent the voltage reversal. Cathode surface area that are placed closed to the membrane are able to promote the rate of oxygen reduction and thus increasing the electricity generation. Deducing from the experimental results, the increment of cathode area reduces the internal resistance which indirectly increased the performance of S-MFC. The reduction of surface area also leads to a faster substrate depletion rate. A maximum performance with power density of 2.867mW was observed and coulombic efficiency of 64.63% was achieved with 0.01m^2 of cathode surface area. This indicates that by implementing a wider surface area of cathode yields positive impacts on the performance of S-MFC power generation.

Acknowledgements

The author gratefully acknowledges the financial support from the Research Management Centre, Universiti Tun Hussein Onn Malaysia (UTHM) under the approved Grant of U957 and Research Fund E15501.

References

[1] P. Mazidi, G. N. Baltas, M. Eliassi, and P. Rodriguez, "A Model for Flexibility Analysis of RESS with Electric Energy Storage and Reserve," *7th International IEEE Conference on Renewable Energy Research and Applications, ICRERA 2018*, vol. 5, pp. 1004–1009, 2018.

[2] T. Sakagami, Y. Shimizu, and H. Kitano, "Exchangeable batteries for micro EVs and renewable energy," *2017 6th International Conference on Renewable Energy Research and Applications, ICRERA 2017*, vol. 2017-Janua, pp. 701–705, 2017.

[3] O. T. Winarno, Y. Alwendra, and S. Mujiyanto, "Policies and strategies for renewable energy development in Indonesia," *2016 IEEE International Conference on Renewable Energy Research and Applications, ICRERA 2016*, vol. 5, pp. 270–272, 2017.

[4] K. D. Mercado, J. Jimenez, and M. C. G. Quintero, "Hybrid renewable energy system based on intelligent optimization techniques," *2016 IEEE International Conference on Renewable Energy Research and Applications (ICRERA)*, 2016.

[5] A. Harrouz, M. Abbes, I. Colak, and K. Kayisli, "Smart grid and renewable energy in Algeria," *2017 IEEE 6th International Conference on Renewable Energy Research and Applications (ICRERA)*, 2017.

[6] L. M. Tender, S. A. Gray, E. Groveman, D. A. Lowy, P. Kauffman, J. Melhado, R. C. Tyce, D. Flynn, R. Petrecca, and J. Dobarro, "The first demonstration of a microbial fuel cell as a viable power supply: Powering a meteorological buoy," *Journal of Power Sources*, vol. 179, no. 2, pp. 571–575, 2008.

[7] H. C. Teng, B. C. Kok, C. Uttraphan, and M. H. Yee, "A Review on Energy Harvesting Potential from Living Plants : Future Energy Resource," *International Journal Of Renewable Energy Research*, vol. 8, no. 4, pp. 2598–2614, 2018.

[8] N. Kaku, N. Yonezawa, Y. Kodama, and K. Watanabe, "Plant/microbe cooperation for electricity generation in a rice paddy field," *Applied Microbiology and Biotechnology*, vol. 79, no. 1, pp. 43–49, 2008.

[9] R. A. Timmers, D. P. B. T. B. Strik, H. V. M. Hamelers, and C. J. N. Buisman, "Electricity generation by a novel design tubular plant microbial fuel cell," *Biomass and Bioenergy*, vol. 51, pp. 60–67, 2013.

[10] T. H. Cheng, K. B. Ching, C. Uttraphan, and Y. M. Heong, "Continuous Monitoring and Analysis of Pandanus Amaryllifolius Microbial Fuel Cell Power Generation in Daily Solar Radiation," *International Journal of New Innovation in Engineering and Technology*, vol. 12, no. 1, pp. 93–103, 2019.

[11] T. H. Cheng, K. B. Ching, C. Uttraphan, and Y. M. Heong, "Electrical energy production from plant biomass : an analysis model development for pandanus amaryllifolius plant microbial fuel cell," *International Journal of Electrical Engineering and Computer Science*, vol. 18, no. 3, pp. 1163–1171, 2020.

[12] J. Sun, Y. Hu, Z. Bi, and Y. Cao, "Improved performance of air-cathode single-chamber microbial fuel cell for wastewater treatment using microfiltration membranes and multiple sludge inoculation," *Journal of Power Sources*, vol. 187, no. 2, pp. 471–479, 2009.

[13] B. E. Logan and J. M. Regan, "Electricity-producing bacterial communities in microbial fuel cells," *Trends in Microbiology*, vol. 14, no. 12, pp. 512–518, 2006.

[14] L. D. Schamphelaire, L. V. D. Bossche, H. S. Dang, M. Höfte, N. Boon, K. Rabaey, and W. Verstraete, "Microbial Fuel Cells Generating Electricity from Rhizodeposits of Rice Plants," *Environmental Science & Technology*, vol. 42, no. 8, pp. 3053–3058, 2008.

[15] B. Lóránt, M. Gyalai-Korpos, I. Goryanin, and G. M. Tardy, "Single chamber air–cathode microbial fuel cells as biosensors for determination of biodegradable organics," *Biotechnology Letters*, vol. 4, pp. 555–563, 2019.

[16] J. Chouler, G. A. Padgett, P. J. Cameron, K. Preuss,

M.-M. Titirici, I. Ieropoulos, and M. D. Lorenzo, "Towards effective small scale microbial fuel cells for energy generation from urine," *Electrochimica Acta*, vol. 192, pp. 89–98, 2016.

[17] A. Fujinaga, K. Tei, H. Ozaki, R. Takanami, and S. Taniguchi, "Evaluation of the Effect of Graphite Powder in Decreasing the Internal Resistance for Microbial Fuel Cell Using Soil," *Journal of Water and Environment Technology*, vol. 14, no. 3, pp. 141–148, 2016.

[18] N. Jannelli, R. Anna Nastro, V. Cigolotti, M. Minutillo, and G. Falcucci, "Low pH, high salinity: Too much for microbial fuel cells?," *Applied Energy*, vol. 192, pp. 543–550, 2017.

[19] X. Li, X. Wang, Q. Zhao, L. Wan, Y. Li, and Q. Zhou, "Carbon fiber enhanced bioelectricity generation in soil microbial fuel cells," *Biosensors and Bioelectronics*, vol. 85, pp. 135–141, 2016.

[20] Z. Chen, Y. chao Huang, J. hong Liang, F. Zhao, and Y. guan Zhu, "A novel sediment microbial fuel cell with a biocathode in the rice rhizosphere," *Bioresource Technology*, vol. 108, pp. 55–59, 2012.

[21] Z. He, H. Shao, and L. T. Angenent, "Increased power production from a sediment microbial fuel cell with a rotating cathode," *Biosensors and Bioelectronics*, vol. 22, no. 12, pp. 3252–3255, 2007.

[22] S. Venkata Mohan, G. Mohanakrishna, and P. Chiranjeevi, "Sustainable power generation from floating macrophytes based ecological microenvironment through embedded fuel cells along with simultaneous wastewater treatment," *Bioresource Technology*, vol. 102, no. 14, pp. 7036–7042, 2011.

[23] R. Nitisoravut and R. Regmi, "Plant microbial fuel cells: A promising biosystems engineering," *Renewable and Sustainable Energy Reviews*, vol. 76, no. September 2016, pp. 81–89, 2017.

[24] J. M. Pisciotta, Z. Zaybak, D. F. Call, J. Y. Nam, and B. E. Logan, "Enrichment of microbial electrolysis cell biocathodes from sediment microbial fuel cell bioanodes," *Applied and Environmental Microbiology*, vol. 78, no. 15, pp. 5212–5219, 2012.

[25] Y. Yang, L. Yan, J. Song, and M. Xu, "Optimizing the electrode surface area of sediment microbial fuel cells," *RSC Advances*, vol. 8, no. 45, pp. 25319–25324, 2018.

[26] S. Chen, B. Chen, and B. D. Fath, "Assessing the cumulative environmental impact of hydropower construction on river systems based on energy network model," *Renewable and Sustainable Energy Reviews*, vol. 42, no. 19, pp. 78–92, 2015.

[27] Y. Fan, H. Hu, and H. Liu, "Enhanced Coulombic efficiency and power density of air-cathode microbial fuel cells with an improved cell configuration," *Journal of Power Sources*, vol. 171, no. 2, pp. 348–354, 2007.

[28] J. Li, H. Li, Q. Fu, Q. Liao, X. Zhu, H. Kobayashi, and D. Ye, "Voltage reversal causes bioanode corrosion in microbial fuel cell stacks," *International Journal of Hydrogen Energy*, vol. 42, no. 45, pp. 27649–27656, 2017.

[29] T. Ewing, P. T. Ha, and H. Beyenal, "Evaluation of long-term performance of sediment microbial fuel cells and the role of natural resources," *Applied Energy*, vol. 192, pp. 490–497, 2017.

[30] M. Devasahayam and S. A. Masih, "Microbial fuel cells demonstrate high coulombic efficiency applicable for water remediation," *Indian Journal of Experimental Biology*, vol. 50, no. 6, pp. 430–438, 2012.

[31] H. Lin, S. Wu, and J. Zhu, "Modeling power generation and energy efficiencies in air-cathode microbial fuel cells based on Freter Equations," *Applied Sciences (Switzerland)*, vol. 8, no. 10, pp. 1–16, 2018.